

Oxidation resistance of Ni-toughened Al_2O_3

T.C. Wang, R.Z. Chen, W.H. Tuan*

Institute of Materials Science and Engineering, National Taiwan University, Taipei 106, Taiwan, ROC

Received 16 November 2001; accepted 16 June 2002

Abstract

Adding nickel inclusions into alumina can enhance its strength and toughness. However, the oxidation resistance of alumina is degraded due to the presence of metallic nickel. In the present study, the oxidation kinetics of Ni-toughened Al_2O_3 in the temperature region from 1000 to 1300 °C are investigated. In the $\text{Al}_2\text{O}_3/\text{Ni}$ composites, the Ni inclusions are isolated to each other within the Al_2O_3 matrix as the Ni content is less than 15 vol.%. The oxidation of the composites is mainly a diffusional process, nickel ions diffuse out and oxygen ions diffuse in. A dense NiAl_2O_4 spinel is formed on the surface of the composite after oxidation. The oxidation rate constants of the alumina incorporated with isolated Ni inclusions are in a comparable range with those of hot-pressed silicon nitride.

© 2002 Elsevier Science Ltd. All rights reserved.

Keywords: Al_2O_3 ; $\text{Al}_2\text{O}_3\text{-Ni}$; Composite; Ni; Oxidation

1. Introduction

The potential of using alumina for engineering applications is high for its availability, high electrical resistance and chemical inertness. However, the brittleness of alumina limits its applications. To cope with this handicap, one of the common approaches is to incorporate a toughening agent to interact with the propagating crack. As more energy is needed to propagate a crack, the resistance of alumina to catastrophic failure is then enhanced. Many toughening agents, either ceramics or metals, have been used to improve the toughness of alumina; many of them are effective. Among them, metallic nickel has attracted much attention recently. One of the reasons is that the mechanical properties of alumina are indeed improved by adding nickel. Several examples^{1–4} are listed in Table 1. These studies indicated that both the strength and toughness of alumina could be significantly improved through the addition of Ni inclusions. Furthermore, since a pressureless sintering technique can be used to consolidate the Ni-toughened Al_2O_3 , the economic potential of the composites is high.

Though the oxidation resistance of nickel is superb among metals, the addition of nickel inclusions to alumina degrades its natural oxidation resistance. The oxidation behaviour of the Ni-toughened Al_2O_3 needs to be characterized before the potential of the composites for engineering applications can be fully realized. In the present study, the oxidation behaviour of Ni-toughened Al_2O_3 is therefore investigated.

2. Experimental procedures

The $\text{Al}_2\text{O}_3/\text{Ni}$ composites were prepared with a selective reduction process as that developed by Tuan and Brook.⁵ A brief description of the preparation procedures is given here. An alumina (TM-DAR, Taimei Chem. Co. Ltd., Japan) powder was ball milled together with various amounts of nickel oxide (NiO, Johnson Matthey Co., USA) powder in ethyl alcohol for 24 h. The grinding media used were zirconia balls. The slurry of the powder mixtures was dried with a rotary evaporator. The dried lumps were crushed and passed through a #150 plastic sieve. Powder compacts with the dimensions of 7×6×50 mm were formed by pressing uniaxially at 44 MPa. The sintering was carried out in a box furnace at 1600 °C for 1 h in air. The heating rate and cooling rate were 5 °C/min. The green compacts were placed within a covered

* Corresponding author. Tel.: +886-2-2365-9800; fax: +886-2-2363-4562.

E-mail address: tuan@ccms.ntu.edu.tw (W.H. Tuan).

graphite crucible. A reducing atmosphere, carbon monoxide, was generated during sintering. The nickel oxide particles were thus reduced to result in nickel inclusions during sintering; the alumina, nevertheless, remained stable. The composition investigated in the present study is shown in Table 2. The final density of the specimens was determined by the Archimedes method. The solubility between the materials used in the present study was low; the relative density of the sintered composites was estimated by using the theoretical density of 3980 kg/m³ for Al₂O₃ and 8900 kg/m³ for Ni. The polished specimens were thermally etched at 1500 °C for 0.5 h to reveal the grain boundaries of matrix grains. Microstructural characterization used scanning electron microscopy (SEM). The volume fraction of Ni after sintering was determined by counting manually the point fraction of nickel inclusions from SEM micrographs. To ensure the accuracy of the data, more than five SEM micrographs were used. The size of Al₂O₃ grains and of Ni inclusions was determined by using the line intercept technique. More than 300 Al₂O₃ grains and 200 Ni inclusions were counted.

The sintered specimens were machined longitudinally with a 325 grit resin-bonded diamond wheel at a depth of 5 µm/pass. The final dimensions of the specimens were 3×4×~36 mm. The fired specimens were then cut into small rectangular specimens with the dimensions of 3×4×10 mm. The specimens were submerged in an ultrasonic bath of acetone for 5 min, and then dried in an oven at 120 °C for 3 h. The dried specimens were

cooled down slowly in a vacuum chamber (10⁻² torr) to room temperature prior to weight measurement. The oxidation was carried out in a box furnace at 1000, 1100, 1190 and 1300 °C for up to 1000 h. The heating rate of the oxidation test was 10 °C/min. After the specimen was oxidized for a pre-determined time, the specimen was cooled down to a temperature around 200 °C with a cooling rate of 10 °C/min, then drawn from the furnace and placed into a vacuum chamber and left until room temperature. One specimen was oxidized only once to avoid any thermal shock effect. The extent of oxidation, weight gain hereafter, was expressed by the weight change per unit area.

Phase identification was performed by X-ray diffractometry (XRD) with CuKα radiation. Grinding with diamond paste to 3 µm and polishing with silica suspension to 0.05 µm exposed the cross section of the oxidized specimens. Care was taken to avoid tensile stress applied on the oxidized surface during grinding and polishing. The atomic distribution within the oxidized specimens was characterized with electron probe microanalysis (EPMA). The interconnectivity of nickel particles within Al₂O₃ matrix was determined by measuring the electrical resistance.

3. Results and discussion

XRD analyses (Figs. 1 and 2), detect only α-Al₂O₃ and cubic-Ni in the as-sintered specimens. Table 2

Table 1
Reported values for the strength and toughness of Ni-toughened Al₂O₃

| Composition | Relative density (%) | Strength (MPa) | Toughness (MPa m ^{0.5}) | Densification techniques | References |
|--|----------------------|----------------|-----------------------------------|--------------------------|------------|
| Al ₂ O ₃ + 4.7 vol.%Ni | 97 | – | 5.5 | Hot-pressing | 1 |
| Al ₂ O ₃ + 5 vol.%Ni | ~100 | 1090 | 3.5 | Hot-pressing | 2 |
| Al ₂ O ₃ + 35 vol.%Ni | 97 | 613 | 12.1 | Reactive hot pressing | 3 |
| Al ₂ O ₃ + 13 vol.%Ni | 98 | 428 | 6.5 | Pressureless sintering | 4 |

Table 2
The nickel content, relative density, size of matrix grains and of inclusions, and electrical resistivity of the Al₂O₃/Ni composites

| Composition | Nickel content after sintering ^a (vol.%) | Relative density (%) | Al ₂ O ₃ matrix grains ^b (µm) | Ni inclusions ^b (µm) | Electrical resistivity (Ω-cm) |
|---|---|----------------------|--|---------------------------------|-------------------------------|
| Al ₂ O ₃ | 0 | 98.2 | 10.9 | – | 6×10 ¹³ |
| Al ₂ O ₃ + 5 vol.%Ni | 4.7 | 99.6 | 6.6 | 2.4 | 4×10 ¹² |
| Al ₂ O ₃ + 7.5 vol.%Ni | 6.7 | 98.7 | 4.6 | 2.6 | 3×10 ¹² |
| Al ₂ O ₃ + 10 vol.%Ni | 8.7 | 99.1 | 4.4 | 2.9 | 4×10 ¹⁰ |
| Al ₂ O ₃ + 12.5 vol.%Ni | 10.8 | 97.6 | 4.3 | 3.7 | 3×10 ¹² |
| Al ₂ O ₃ + 15 vol.%Ni | 12.9 | 98.1 | 3.8 | 4.9 | 5×10 ¹¹ |

^a Determined by point counting.

^b Determined by line intercept method.

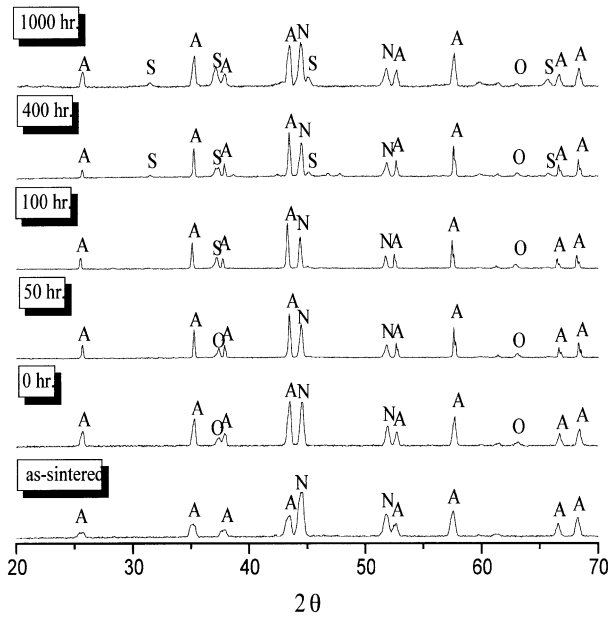


Fig. 1. XRD patterns of the $\text{Al}_2\text{O}_3/12.5\%\text{Ni}$ composites oxidized at 1000°C for various times (A = Al_2O_3 , N = Ni, O = NiO, S = NiAl_2O_4).

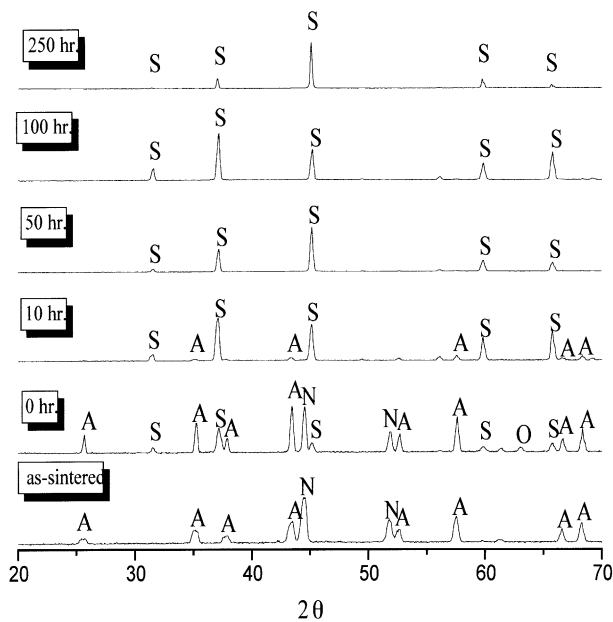


Fig. 2. XRD patterns of the $\text{Al}_2\text{O}_3/12.5\%\text{Ni}$ composites oxidized at 1300°C for various times (A = Al_2O_3 , N = Ni, O = NiO, S = NiAl_2O_4).

shows the nickel content, relative density, the size of Al_2O_3 matrix grains and of Ni inclusions of the composites prepared in the present study. The sintering temperature is higher than the melting point of Ni, 1453°C . The nickel content in the sintered composites is thus lower than that in the starting composition due to the vaporization of nickel during sintering at 1600°C .⁵ The electrical resistivity of $\text{Al}_2\text{O}_3/\text{Ni}$ composites is higher than $10^{10}\ \Omega\text{-cm}$, indicating that Ni inclusions are isolated to each other within the matrix.

cm, indicating that Ni inclusions are isolated to each other within the matrix.

Fig. 1 also shows the XRD patterns of the $\text{Al}_2\text{O}_3/\text{Ni}$ composites oxidized at 1000°C for up to 1000 h. Nickel oxide first appeared on the composite surface as the composite is heated to 1000°C without any dwell. After the specimen oxidized at 1000°C for 100 h, nickel aluminate spinel (NiAl_2O_4) is formed. The NiO and NiAl_2O_4 then co-existed on the surface until the specimen oxidized at 1000°C for 1000 h. However, the amount of spinel increases with the increase of oxidation time; the amount of nickel oxide shows, nevertheless, opposite trend.

Fig. 2 shows the XRD patterns of the $\text{Al}_2\text{O}_3/\text{Ni}$ composites oxidized at 1300°C for various times. Apart from Al_2O_3 and Ni, NiO and NiAl_2O_4 are found on the surface of the specimen heated at 1300°C for 0 h. Then, Ni and NiO are disappeared from the surface; the amount of NiAl_2O_4 increased instead as the oxidation time is longer than 10 h. Only NiAl_2O_4 is detected on the surface, as the oxidation time is longer than 50 h.

XRD analysis suggests that the nickel inclusions exposed on the surface are first oxidized in the beginning of the oxidation at elevated temperature, as



As the oxidation proceeds, NiO can then react with the Al_2O_3 matrix to form NiAl_2O_4 as

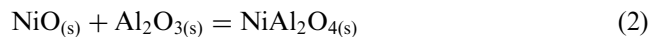


Fig. 3 shows the square of weight gain of the composites as a function of oxidation time. Except the oxidation at a lower temperature, 1000°C , for a shorter time, <100 h, the square of weight gain mainly follows a linear relationship with oxidation time. It suggests that the oxidation process in the beginning is controlled by the interfacial reaction between oxygen gas and metallic nickel, as demonstrated in Eq. (1). As the oxidation proceeds, a diffusion process then controls the oxidation.

Fig. 4 shows typical microstructure of an oxidized composite; the dark phase is alumina, gray phase spinel and brightest phase nickel. Three zones can be distinguished from the cross-section of the oxidized composites. A dense spinel zone is found on the surface region. The second zone from the surface is a region that mixes alumina and spinel. Near the end of the second zone, the residual nickel inclusions surrounded by spinel can be found. The third zone from the surface is a region similar to that of the original composite which composing of a mixture of alumina and nickel, except a small amount of NiAl_2O_4 spinel is also present. The dense surface spinel layer increases in its thickness with the increase of nickel content; it also increases its amount with the increase of oxidation temperature.

From the microstructure observation, the oxidation is found mainly in the surface layer.

For the oxidation of mullite/SiC composites, Lin et al. proposed two types of oxidation mode.⁶ The mode I oxidation is a type that the diffusion of oxygen in matrix is very slow; the oxidation takes place only in the surface region. The mode II oxidation is a type that the

diffusion is relatively fast in matrix. No dense oxidized surface layer was found in such oxidation mode. They found that the oxidation type of mullite/SiC composites was mode I. The resistance of the mullite/SiC composites to oxidation is therefore high. The oxidation of $\text{Al}_2\text{O}_3/\text{Ni}$ composites is mainly a mode I type and mixed with a small amount of mode II type, indicating that the

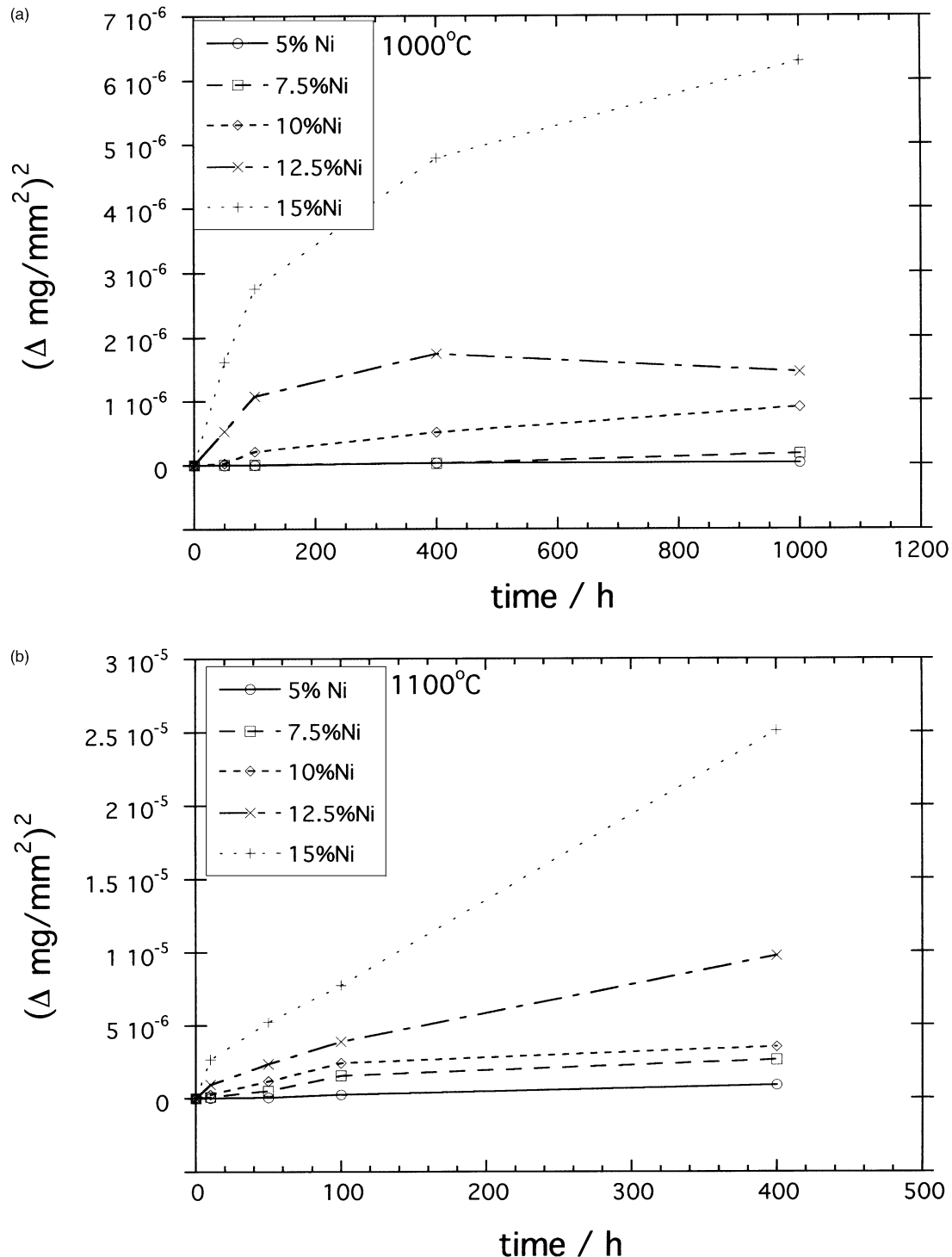


Fig. 3. Square of weight gains as function of oxidation time at (a) 1000 °C, (b) 1100 °C, (c) 1190 °C and (d) 1300 °C.

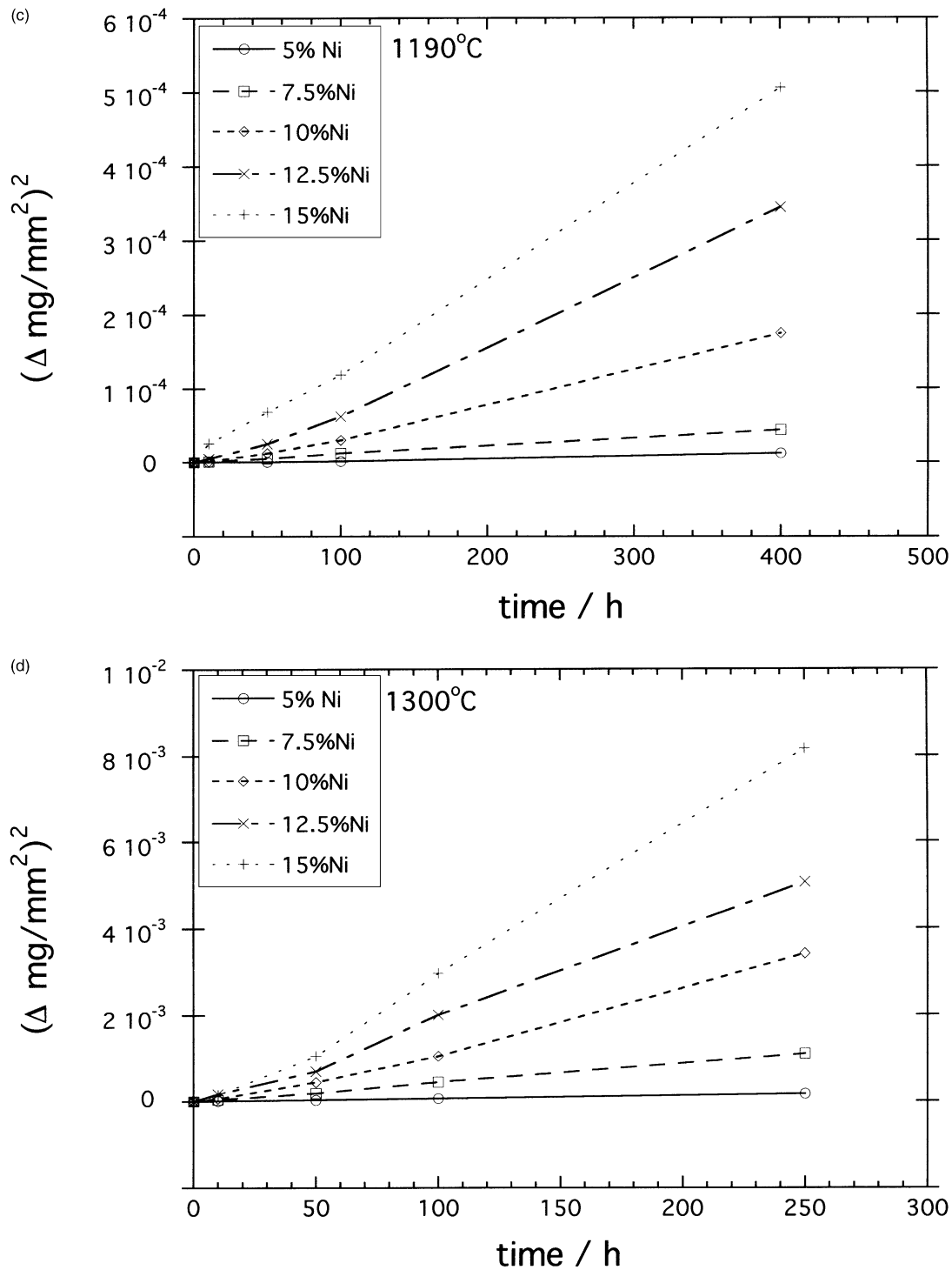


Fig. 3. (continued).

nickel inclusions are also well protected by the alumina matrix.

An EPMA analysis is carried out on an Al₂O₃/12.5%Ni composite which is oxidized at 1190 °C for 400 h (Fig. 5). The detected volume of each electron probe was around 1 μm in diameter in the surface region. Therefore, the EPMA analysis was carried out every

one micrometer from the surface. A total distance of 120 μm was determined. Three distinct zones can be found from Fig. 5. The thickness of the first zone is around 15 μm. The atomic percentage of oxygen, aluminum and nickel remains the same in the zone. The atomic ratio of Ni, Al and O is about 1:2:4 in this zone, which is the molar ratio of NiAl₂O₄. From the XRD,

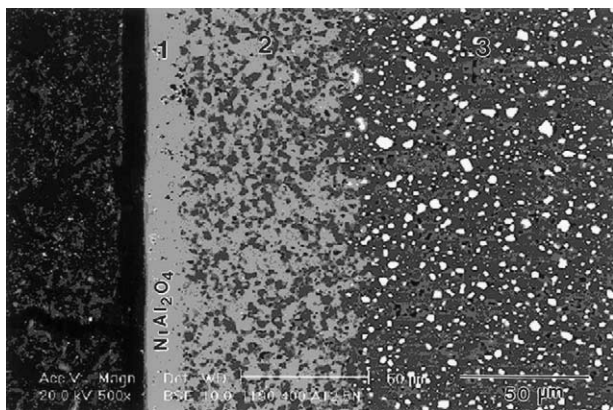


Fig. 4. SEM micrograph of the $\text{Al}_2\text{O}_3/12.5\%\text{Ni}$ composite oxidized at $1190\text{ }^\circ\text{C}$ for 400 h. Three zones are indicated (see text).

EPMA analyses and microstructural observation, it demonstrates that a dense spinel surface layer is formed on the surface of the oxidized composite. The atomic percentage of O, Al and Ni then fluctuates in the second region, around $60\text{ }\mu\text{m}$ thick, indicating the zone is composing of alumina and spinel inclusions. In the third zone, the atomic percentage remains more or less the same unless a nickel particle spotted by the electron probe.

In the temperature range investigated, from 1000 to $1300\text{ }^\circ\text{C}$, the reactants and the product of the reaction (2) are all in their solid state. The solid-state reaction between NiO and Al_2O_3 has been investigated extensively,^{7–11} the reaction was controlled by a counter-diffusion of Al^{+3} and Ni^{+2} ions. For the heat treatment of $\text{Al}_2\text{O}_3/\text{Ni}$ composites in air, the oxidation is also a diffusional

process (Fig. 3). In order to oxidize nickel in Al_2O_3 matrix, oxygen from the surrounding air needs to transport into the interior of the composite. Oxygen thus has to diffuse through the alumina matrix and NiAl_2O_4 , which enclose the Ni inclusions.

Dense NiAl_2O_4 surface layer was always found on the oxidized composites after the oxidation in air. From the reaction (2), one mole Ni reacts with one mole Al_2O_3 to form NiAl_2O_4 . The molar ratio of Al_2O_3 to Ni in the $\text{Al}_2\text{O}_3/\text{Ni}$ composites varies from 1:0.19 to 1:0.58. Since only a small amount of Al_2O_3 , around 0.3 mol, can solute into 1 mole of NiAl_2O_4 in the temperature range from 1000 to $1300\text{ }^\circ\text{C}$;¹² the amount of Ni per unit volume in the composites is not sufficient to convert all Al_2O_3 to NiAl_2O_4 . It indicates that not only oxygen transports inward, but nickel also transports outward during oxidation. Therefore, the oxidation of $\text{Al}_2\text{O}_3/\text{Ni}$ composites is an oxygen ions diffuse in and nickel ions diffuse out process.

In the second zone from the surface, there is no NiO intermediate phase detected at the $\text{NiAl}_2\text{O}_4/\text{Ni}$ interface, indicating that NiO reacts with Al_2O_3 to form NiAl_2O_4 immediately after the formation of NiO. The NiAl_2O_4 remains after its formation at elevated temperature.

The diffusional oxidation process is a thermal activated process, can be expressed as

$$(\Delta W/A)^2 = K_p t \quad (3)$$

where $\Delta W/A$ is the weight change per unit area, K_p the oxidation rate constant, t the oxidation time. The

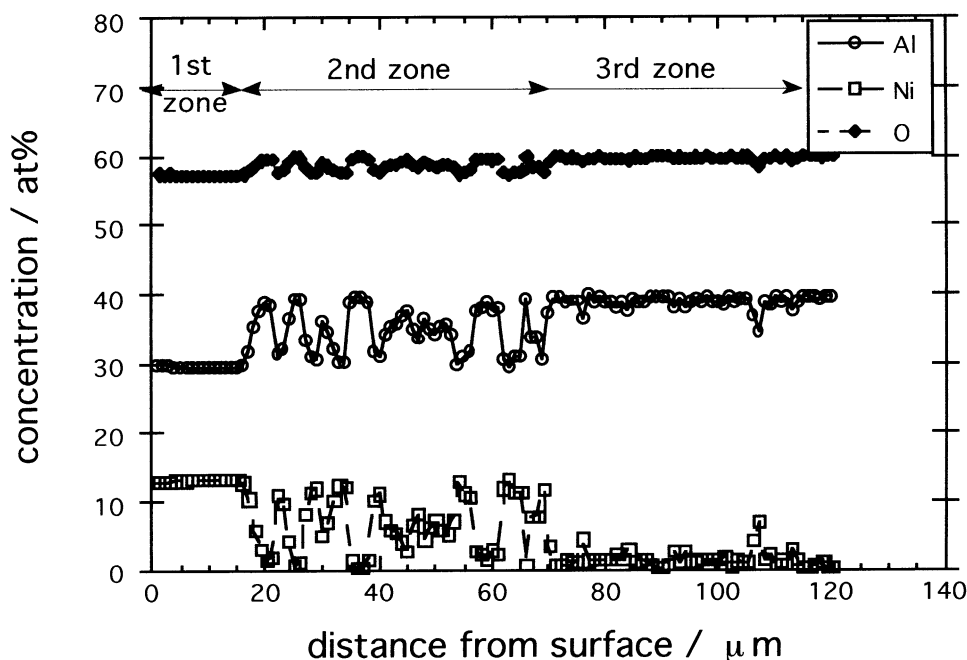


Fig. 5. EPMA analysis corresponds to the cross-section shown in Fig. 4. The EPMA analysis was carried out at every $1\text{ }\mu\text{m}$ from the oxidized surface. Three zones (see text) are indicated.

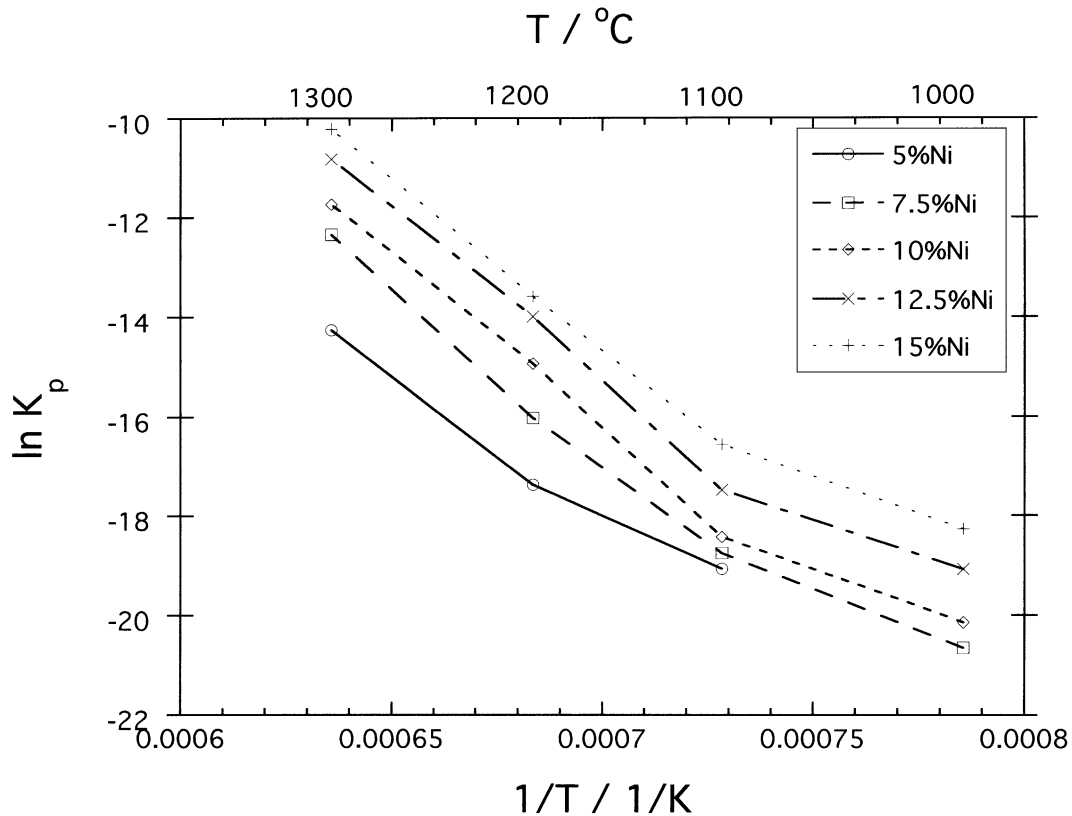


Fig. 6. Oxidation rate constant as function of temperature.

oxidation rate constant can be expressed with an Arrhenius equation as

$$K_p = K_o \exp(-Q/RT) \quad (4)$$

In Eq. (4), K_o is a constant, Q the activation energy, R the gas constant and T the temperature. Fig. 6 shows the oxidation rate constant as a function of the inverse of temperature. The figure demonstrates two regions with different activation energy. The calculated values

Table 3
Activation energy of oxidation in the temperature region from 1000 to 1300 °C

| Composition | Activation energy (kJ/mol) | |
|---|--------------------------------|---------------------------------|
| | Lower temperature ^a | Higher temperature ^b |
| Al ₂ O ₃ + 5 vol.%Ni | 314 | 543 |
| Al ₂ O ₃ + 7.5 vol.%Ni | 275 | 577 |
| Al ₂ O ₃ + 10 vol.%Ni | 249 | 601 |
| Al ₂ O ₃ + 12.5 vol.%Ni | 232 | 598 |
| Al ₂ O ₃ + 15 vol.%Ni | 249 | 570 |
| Average | 267 ± 32 | 578 ± 24 |

^a For the Al₂O₃ + 5 vol.%Ni composite, the lower temperature indicates the temperature region from 1000 to 1200 °C, for other composites from 1000 to 1100 °C.

^b For the Al₂O₃ + 5 vol.%Ni composite, the higher temperature indicates the temperature region from 1200 to 1300 °C, for other composites from 1100C to 1300 °C.

for the activation energies are shown in Table 3. The activation energy of the composite containing 5 vol.%Ni in the temperature region from 1000 to 1200 °C and other composites in the temperature region from 1000 to 1100 °C are varied in a rather narrow range, from 230 to 310 kJ/mol. In the higher temperature range, the activation energy varies from 540 to 600 kJ/mol. The reported values^{8,13–17} for the activation energy of the related systems are collected in Table 4. By comparing the reported values, it suggests that the oxidation at lower temperature is controlled by the diffusion of nickel ion through the grain boundaries of alumina. At higher temperature, the activation energy is close to the value reported for the diffusion of oxygen ion through

Table 4
Reported values for the activation energy in the related systems

| Temperature (K) | Diffusion species | Diffusion path | Activation energy (kJ/mol) | Reference |
|-----------------|-------------------|---|----------------------------|-----------|
| 795–1073 | Ni ²⁺ | NiO, volume | 246 | 13 |
| 795–1073 | Ni ²⁺ | NiO, grain boundary | 193 | 13 |
| 773–1073 | Ni ²⁺ | NiO, volume | 247 | 14 |
| 773–1073 | Ni ²⁺ | NiO, grain boundary | 172 | 14 |
| 773–1073 | Ni ²⁺ | NiO, grain boundary | 179–253 | 15 |
| 1483–1643 | Ni ²⁺ | Al ₂ O ₃ , grain boundary | 264 | 8 |
| 1473–1923 | O ²⁻ | Al ₂ O ₃ , grain boundary | 594 | 16 |
| 1400–2000 | Al ³⁺ | Al ₂ O ₃ , grain boundary | 418 | 17 |

the grain boundaries of alumina. However, a dense NiAl_2O_4 protective layer is formed on the surface as the composites are oxidized at higher temperature. Furthermore, before Ni inclusions are fully consumed by oxygen, dense NiAl_2O_4 surrounds every Ni inclusion. Oxygen ions thus travel within both alumina and spinel phase. The atomic packing of oxygen in Al_2O_3 and NiAl_2O_4 phases is very similar.¹⁸ Therefore, the activation energy of the diffusion of oxygen in NiAl_2O_4 should be very close to that of oxygen in Al_2O_3 . The oxidation at higher temperature is therefore more likely controlled by the diffusion of oxygen ion through both alumina and nickel aluminate spinel.

To compare the natural oxidation resistance of Al_2O_3 , the addition of Ni degrades its oxidation resistance. However, the oxidation resistance of the composites should also compare with other ceramics that are not oxidation free. If we take silicon nitride as the basis for comparison, the reported values for the oxidation rate constant of hot-pressed Si_3N_4 lie between 10^{-10} and 10^{-12} $\text{g}^2 \text{cm}^{-4} \text{s}^{-1}$ from 1300 to 1400 °C.¹⁹ For the $\text{Al}_2\text{O}_3/15\% \text{Ni}$ composite, the strength and toughness are 428 MPa and 6.5 MPam^{0.5}, respectively,⁴ which are higher than those of alumina alone. The electrical resistivity of the composite is as high as 5×10^{11} $\Omega\text{-cm}$, indicating that Ni particles are separated from each other within the alumina matrix. The oxidation rate constant of the composite at 1300 °C is 10^{-10} $\text{g}^2 \text{cm}^{-4} \text{s}^{-1}$, indicating that the nickel inclusions are well protected by the matrix composing of Al_2O_3 and NiAl_2O_4 . The oxidation study on the $\text{Al}_2\text{O}_3/\text{Ni}$ composites suggests that the composites with isolated metallic inclusions are potential material for structural and electrical insulation applications.

4. Conclusions

The oxidation behaviour of $\text{Al}_2\text{O}_3/\text{Ni}$ composites is investigated in the present study. The composites with isolated Ni inclusions were prepared by a pressureless sintering technique. The oxidation is taken place firstly by the interfacial reaction between oxygen gas and the exposed nickel particles on the composite surface. Then, the oxidation is controlled by diffusion. In the beginning of the diffusional oxidation, the amount of NiAl_2O_4 is small; the diffusion of Ni ions through the grain boundaries of Al_2O_3 controls the process. A dense NiAl_2O_4 layer formed on the surface region at this stage. The oxidation is then controlled by the diffusion of oxygen through alumina and nickel aluminate spinel. The oxidation product, NiAl_2O_4 , is dense and protective; the oxidation resistance of the $\text{Al}_2\text{O}_3/\text{Ni}$ composites is thus comparable to that of engineering silicon nitrides.

Acknowledgements

The National Science Council, ROC, supports the present study through the contract number of NSC89–2216-E002–049.

References

1. Breval, E., Deng, Z., Chio, S. and Pantano, C. G., Sol-gel prepared $\text{Al}_2\text{O}_3/\text{Ni}$ composite material I. Microstructure and mechanical properties. *J. Mater. Sci.*, 1992, **27**, 1464–1468.
2. Sekino, T., Nakajima, T., Ueda, S. and Niihara, K., Reduction and sintering of a nickel-dispersed-alumina composite and its properties. *J. Am. Ceram. Soc.*, 1997, **80**, 1139–1148.
3. Fahrenholtz, W. G., Ellerby, D. T. and Loehman, R. E., Al_2O_3 –Ni composites with high strength and fracture toughness. *J. Am. Ceram. Soc.*, 2000, **83**, 1279–1280.
4. Chen, R. Z., Chiu, Y. T. and Tuan, W. H., Toughening alumina with both nickel and zirconia inclusions. *J. Eur. Ceram. Soc.*, 2000, **20**, 1901–1906.
5. Tuan, W. H. and Brook, R. J., Processing of alumina/nickel composites. *J. Eur. Ceram. Soc.*, 1992, **10**, 95–100.
6. Lin, C.-C., Zangvil, A. and Ruh, R., Mode of oxidation in SiC-reinforced mullite/ ZrO_2 composites: oxidation vs depth behavior. *Acta Mater.*, 1999, **47**, 1977–1986.
7. Pettit, F. S., Randklev, E. H. and Eelten, E. J., Formation of NiAl_2O_4 by solid state reaction. *J. Am. Ceram. Soc.*, 1966, **49**, 199–203.
8. Hirota, K. and Komatsu, W., Concurrent measurement of volume, grain boundary and surface diffusion coefficients in the system NiO– Al_2O_3 . *J. Am. Ceram. Soc.*, 1977, **60**, 105–110.
9. Rossi, R. C. and Fulrath, R. M., Epitaxial growth of spinel by reaction in the solid state. *J. Am. Ceram. Soc.*, 1963, **46**, 145–150.
10. Kotula, P. G. and Carter, C. B., Nucleation of solid-state reactions between nickel oxide and aluminum oxide. *J. Am. Ceram. Soc.*, 1995, **78**, 248–250.
11. Elrefaie, F. A. and Smeltzer, W. W., Phase equilibria in the sub-solidus region of the NiO– Al_2O_3 system between 1000 and 1920 °C. *Oxid. Met.*, 1981, **15**, 495–500.
12. Trumble, K. P. and Rühle, M., The thermodynamics of spinel interphase formation at diffusion-bonded Ni/ Al_2O_3 interface. *Acta Metall. Mater.*, 1991, **39**(8), 1915–1924.
13. Aktinson, A. and Taylor, R. I., The diffusion of Ni in the bulk and along dislocations in NiO single crystals. *Phil. Mag. A*, 1979, **39**, 581–595.
14. Aktinson, A. and Taylor, R. I., The diffusion of ^{63}Ni along grain boundaries in nickel oxide. *Phil. Mag. A*, 1981, **43**, 979–998.
15. Kaur, I., Gust, W. and Kozma, L., *Handbook of Grain Interphase Boundary Diffusion Data*. Ziegler Press, Stuttgart, 1989.
16. Johnson, D. L. and Cutler, I. B., Diffusional sintering I, Initial stage models and their applications to shrinkage of powder compacts. *J. Am. Ceram. Soc.*, 1963, **46**, 541–545.
17. Cannon, R. M., Rhodes, W. H. and Heuer, A. H., Plastic deformation of fine-grained alumina (Al_2O_3): I, interfacial-controlled diffusional creep. *J. Am. Ceram. Soc.*, 1980, **63**, 46–53.
18. Simpson, Y. K., McKernan, S. and Carter, C. B., An alumina/spinel interface. *J. Am. Ceram. Soc.*, 1987, **70** (back cover of July issue).
19. Pomeroy, M. and Hampshire, S., Oxidation processes in silicon nitride based ceramics. *Mater. Sci. Eng.*, 1989, **A109**, 389–394.